

Search for third generation vector leptoquarks in $p\bar{p}$ collisions at $\sqrt{s} = 1.96$ TeV

T. Aaltonen,²³ A. Abulencia,²⁴ J. Adelman,¹³ T. Affolder,¹⁰ T. Akimoto,⁵⁵ M. G. Albrow,¹⁷ S. Amerio,⁴³ D. Amidei,³⁵ A. Anastassov,⁵² K. Anikeev,¹⁷ A. Annovi,¹⁹ J. Antos,¹⁴ M. Aoki,⁵⁵ G. Apollinari,¹⁷ T. Arisawa,⁵⁷ A. Artikov,¹⁵ W. Ashmanskas,¹⁷ A. Attal,³ A. Aurisano,⁵³ F. Azfar,⁴² P. Azzi-Bacchetta,⁴³ P. Azzurri,⁴⁶ N. Bacchetta,⁴³ W. Badgett,¹⁷ A. Barbaro-Galtieri,²⁹ V. E. Barnes,⁴⁸ B. A. Barnett,²⁵ S. Baroian,⁷ V. Bartsch,³¹ G. Bauer,³³ P.-H. Beauchemin,³⁴ F. Bedeschi,⁴⁶ S. Behari,²⁵ G. Bellettini,⁴⁶ J. Bellinger,⁵⁹ A. Belloni,³³ D. Benjamin,¹⁶ A. Beretvas,¹⁷ J. Beringer,²⁹ T. Berry,³⁰ A. Bhatti,⁵⁰ M. Binkley,¹⁷ D. Bisello,⁴³ I. Bizjak,³¹ R. E. Blair,² C. Blocker,⁶ B. Blumenfeld,²⁵ A. Bocci,¹⁶ A. Bodek,⁴⁹ V. Boisvert,⁴⁹ G. Bolla,⁴⁸ A. Bolshov,³³ D. Bortoletto,⁴⁸ J. Boudreau,⁴⁷ A. Boveia,¹⁰ B. Brau,¹⁰ L. Brigliadori,⁵ C. Bromberg,³⁶ E. Brubaker,¹³ J. Budagov,¹⁵ H. S. Budd,⁴⁹ S. Budd,²⁴ K. Burkett,¹⁷ G. Busetto,⁴³ P. Bussey,²¹ A. Buzatu,³⁴ K. L. Byrum,² S. Cabrera,^{16,q} M. Campanelli,²⁰ M. Campbell,³⁵ F. Canelli,¹⁷ A. Canepa,⁴⁵ S. Carrillo,^{18,i} D. Carlsmith,⁵⁹ R. Carosi,⁴⁶ S. Carron,³⁴ B. Casal,¹¹ M. Casarsa,⁵⁴ A. Castro,⁵ P. Catastini,⁴⁶ D. Cauz,⁵⁴ M. Cavalli-Sforza,³ A. Cerri,²⁹ L. Cerrito,^{31,m} S. H. Chang,²⁸ Y. C. Chen,¹ M. Chertok,⁷ G. Chiarelli,⁴⁶ G. Chlachidze,¹⁷ F. Chlebana,¹⁷ I. Cho,²⁸ K. Cho,²⁸ D. Chokheli,¹⁵ J. P. Chou,²² G. Choudalakis,³³ S. H. Chuang,⁵² K. Chung,¹² W. H. Chung,⁵⁹ Y. S. Chung,⁴⁹ M. Cilijak,⁴⁶ C. I. Ciobanu,²⁴ M. A. Ciocci,⁴⁶ A. Clark,²⁰ D. Clark,⁶ M. Coca,¹⁶ G. Compostella,⁴³ M. E. Convery,⁵⁰ J. Conway,⁷ B. Cooper,³¹ K. Copic,³⁵ M. Cordelli,¹⁹ G. Cortiana,⁴³ F. Crescioli,⁴⁶ C. Cuenca Almenar,^{7,q} J. Cuevas,^{11,l} R. Culbertson,¹⁷ J. C. Cully,³⁵ S. DaRonco,⁴³ M. Datta,¹⁷ S. D'Auria,²¹ T. Davies,²¹ D. Dagenhart,¹⁷ P. de Barbaro,⁴⁹ S. De Cecco,⁵¹ A. Deisher,²⁹ G. De Lentdecker,^{49,c} G. De Lorenzo,³ M. Dell'Orso,⁴⁶ F. Delli Paoli,⁴³ L. Demortier,⁵⁰ J. Deng,¹⁶ M. Deninno,⁵ D. De Pedis,⁵¹ P. F. Derwent,¹⁷ G. P. Di Giovanni,⁴⁴ C. Dionisi,¹⁷ B. Di Ruzza,⁵⁴ J. R. Dittmann,⁴ M. D'Onofrio,³ C. Dörr,²⁶ S. Donati,⁴⁶ P. Dong,⁸ J. Donini,⁴³ T. Dorigo,⁴³ S. Dube,⁵² J. Efron,³⁹ R. Erbacher,⁷ D. Errede,²⁴ S. Errede,²⁴ R. Eusebi,¹⁷ H. C. Fang,²⁹ S. Farrington,³⁰ I. Fedorko,⁴⁶ W. T. Fedorko,¹³ R. G. Feild,⁶⁰ M. Feindt,²⁶ J. P. Fernandez,³² R. Field,¹⁸ G. Flanagan,⁴⁸ R. Forrest,⁷ S. Forrester,⁷ M. Franklin,²² J. C. Freeman,²⁹ I. Furic,¹³ M. Gallinaro,⁵⁰ J. Galyardt,¹² J. E. Garcia,⁴⁶ F. Garbersson,¹⁰ A. F. Garfinkel,⁴⁸ C. Gay,⁶⁰ H. Gerberich,²⁴ D. Gerdes,³⁵ S. Giagu,⁵¹ P. Giannetti,⁴⁶ K. Gibson,⁴⁷ J. L. Gimmell,⁴⁹ C. Ginsburg,¹⁷ N. Giokaris,^{15,a} M. Giordani,⁵⁴ P. Giromini,¹⁹ M. Giunta,⁴⁶ G. Giurgiu,²⁵ V. Glagolev,¹⁵ D. Glenzinski,¹⁷ M. Gold,³⁷ N. Goldschmidt,¹⁷ J. Goldstein,^{42,b} A. Golossanov,¹⁷ G. Gomez,¹¹ G. Gomez-Ceballos,³³ M. Goncharov,⁵³ O. González,³² I. Gorelov,³⁷ A. T. Goshaw,¹⁶ K. Goulianos,⁵⁰ A. Gresele,⁴³ S. Grinstein,²² C. Grosso-Pilcher,¹³ R. C. Group,¹⁷ U. Grundler,²⁴ J. Guimaraes da Costa,²² Z. Gunay-Unalan,³⁶ C. Haber,²⁹ K. Hahn,³³ S. R. Hahn,¹⁷ E. Halkiadakis,⁵² A. Hamilton,²⁰ B.-Y. Han,⁴⁹ J. Y. Han,⁴⁹ R. Handler,⁵⁹ F. Happacher,¹⁹ K. Hara,⁵⁵ D. Hare,⁵² M. Hare,⁵⁶ S. Harper,⁴² R. F. Harr,⁵⁸ R. M. Harris,¹⁷ M. Hartz,⁴⁷ K. Hatakeyama,⁵⁰ J. Hauser,⁸ C. Hays,⁴² M. Heck,²⁶ A. Heijboer,⁴⁵ B. Heinemann,²⁹ J. Heinrich,⁴⁵ C. Henderson,³³ M. Herndon,⁵⁹ J. Heuser,²⁶ D. Hidas,¹⁶ C. S. Hill,^{10,b} D. Hirschbuehl,²⁶ A. Hocker,¹⁷ A. Holloway,²² S. Hou,¹ M. Houlden,³⁰ S.-C. Hsu,⁹ B. T. Huffman,⁴² R. E. Hughes,³⁹ U. Husemann,⁶⁰ J. Huston,³⁶ J. Incandela,¹⁰ G. Introzzi,⁴⁶ M. Iori,⁵¹ A. Ivanov,⁷ B. Iyutin,³³ E. James,¹⁷ D. Jang,⁵² B. Jayatilaka,¹⁶ D. Jeans,⁵¹ E. J. Jeon,²⁸ S. Jindariani,¹⁸ W. Johnson,⁷ M. Jones,⁴⁸ K. K. Joo,²⁸ S. Y. Jun,¹² J. E. Jung,²⁸ T. R. Junk,²⁴ T. Kamon,⁵³ P. E. Karchin,⁵⁸ Y. Kato,⁴¹ Y. Kemp,²⁶ R. Kephart,¹⁷ U. Kerzel,²⁶ V. Khotilovich,⁵³ B. Kilminster,³⁹ D. H. Kim,²⁸ H. S. Kim,²⁸ J. E. Kim,²⁸ M. J. Kim,¹⁷ S. B. Kim,²⁸ S. H. Kim,⁵⁵ Y. K. Kim,¹³ N. Kimura,⁵⁵ L. Kirsch,⁶ S. Klimenko,¹⁸ M. Klute,³³ B. Knuteson,³³ B. R. Ko,¹⁶ K. Kondo,⁵⁷ D. J. Kong,²⁸ J. Konigsberg,¹⁸ A. Korytov,¹⁸ A. V. Kotwal,¹⁶ A. C. Kraan,⁴⁵ J. Kraus,²⁴ M. Kreps,²⁶ J. Kroll,⁴⁵ N. Krumnack,⁴ M. Kruse,¹⁶ V. Krutelyov,¹⁰ T. Kubo,⁵⁵ S. E. Kuhlmann,² T. Kuhr,²⁶ N. P. Kulkarni,⁵⁸ Y. Kusakabe,⁵⁷ S. Kwang,¹³ A. T. Laasanen,⁴⁸ S. Lai,³⁴ S. Lami,⁴⁶ S. Lammel,¹⁷ M. Lancaster,³¹ R. L. Lander,⁷ K. Lannon,³⁹ A. Lath,⁵² G. Latino,⁴⁶ I. Lazzizzera,⁴³ T. LeCompte,² J. Lee,⁴⁹ J. Lee,²⁸ Y. J. Lee,²⁸ S. W. Lee,^{53,o} R. Lefèvre,²⁰ N. Leonardo,³³ S. Leone,⁴⁶ S. Levy,¹³ J. D. Lewis,¹⁷ C. Lin,⁶⁰ C. S. Lin,¹⁷ M. Lindgren,¹⁷ E. Lipeles,⁹ A. Lister,⁷ D. O. Litvintsev,¹⁷ T. Liu,¹⁷ N. S. Lockyer,⁴⁵ A. Loginov,⁶⁰ M. Loreti,⁴³ R.-S. Lu,¹ D. Lucchesi,⁴³ P. Lujan,²⁹ P. Lukens,¹⁷ G. Lungu,¹⁸ L. Lyons,⁴² J. Lys,²⁹ R. Lysak,¹⁴ E. Lytken,⁴⁸ P. Mack,²⁶ D. MacQueen,³⁴ R. Madrak,¹⁷ K. Maeshima,¹⁷ K. Makhoul,³³ T. Maki,²³ P. Maksimovic,²⁵ S. Malde,⁴² S. Malik,³¹ G. Manca,³⁰ A. Manousakis,^{15,a} F. Margaroli,⁵ R. Marginean,¹⁷ C. Marino,²⁶ C. P. Marino,²⁴ A. Martin,⁶⁰ M. Martin,²⁵ V. Martin,^{21,g} M. Martínez,³ R. Martínez-Ballarín,³² T. Maruyama,⁵⁵ P. Mastrandrea,⁵¹ T. Masubuchi,⁵⁵ H. Matsunaga,⁵⁵ M. E. Mattson,⁵⁸ R. Mazini,³⁴ P. Mazzanti,⁵ K. S. McFarland,⁴⁹ P. McIntyre,⁵³ R. McNulty,^{30,f} A. Mehta,³⁰ P. Mehtala,²³ S. Menzemer,^{11,h} A. Menzione,⁴⁶ P. Merkel,⁴⁸ C. Mesropian,⁵⁰ A. Messina,³⁶ T. Miao,¹⁷ N. Miladinovic,⁶ J. Miles,³³ R. Miller,³⁶ C. Mills,¹⁰ M. Milnik,²⁶ A. Mitra,¹ G. Mitselmakher,¹⁸ A. Miyamoto,²⁷ S. Moed,²⁰ N. Moggi,⁵ B. Mohr,⁸ C. S. Moon,²⁸ R. Moore,¹⁷ M. Morello,⁴⁶ P. Movilla Fernandez,²⁹ J. Mülmenstädt,²⁹ A. Mukherjee,¹⁷ Th. Muller,²⁶ R. Mumford,²⁵ P. Murat,¹⁷ M. Mussini,⁵ J. Nachtman,¹⁷ A. Nagano,⁵⁵ J. Naganoma,⁵⁷ K. Nakamura,⁵⁵ I. Nakano,⁴⁰ A. Napier,⁵⁶ V. Necula,¹⁶ C. Neu,⁴⁵ M. S. Neubauer,⁹ J. Nielsen,^{29,n} L. Nodulman,² O. Norniella,³ E. Nurse,³¹ S. H. Oh,¹⁶

Y. D. Oh,²⁸ I. Oksuzian,¹⁸ T. Okusawa,⁴¹ R. Oldeman,³⁰ R. Orava,²³ K. Osterberg,²³ C. Pagliarone,⁴⁶ E. Palencia,¹¹ V. Papadimitriou,¹⁷ A. Papaikonomou,²⁶ A. A. Paramonov,¹³ B. Parks,³⁹ S. Pashapour,³⁴ J. Patrick,¹⁷ G. Pauletta,⁵⁴ M. Paulini,¹² C. Paus,³³ D. E. Pellett,⁷ A. Penzo,⁵⁴ T. J. Phillips,¹⁶ G. Piacentino,⁴⁶ J. Piedra,⁴⁴ L. Pinera,¹⁸ K. Pitts,²⁴ C. Plager,⁸ L. Pondrom,⁵⁹ X. Portell,³ O. Poukhov,¹⁵ N. Pounder,⁴² F. Prakoshyn,¹⁵ A. Pronko,¹⁷ J. Proudfoot,² F. Ptohos,^{19,e} G. Punzi,⁴⁶ J. Pursley,²⁵ J. Rademacker,^{42,b} A. Rahaman,⁴⁷ V. Ramakrishnan,⁵⁹ N. Ranjan,⁴⁸ I. Redondo,³² B. Reisert,¹⁷ V. Rekovic,³⁷ P. Renton,⁴² M. Rescigno,⁵¹ S. Richter,²⁶ F. Rimondi,⁵ L. Ristori,⁴⁶ A. Robson,²¹ T. Rodrigo,¹¹ E. Rogers,²⁴ S. Rolli,⁵⁶ R. Roser,¹⁷ M. Rossi,⁵⁴ R. Rossin,¹⁰ P. Roy,³⁴ A. Ruiz,¹¹ J. Russ,¹² V. Rusu,¹³ H. Saarikko,²³ A. Safonov,⁵³ W. K. Sakumoto,⁴⁹ G. Salamanna,⁵¹ O. Saltó,³ L. Santi,⁵⁴ S. Sarkar,⁵¹ L. Sartori,⁴⁶ K. Sato,¹⁷ P. Savard,³⁴ A. Savoy-Navarro,⁴⁴ T. Scheidle,²⁶ P. Schlabach,¹⁷ E. E. Schmidt,¹⁷ M. P. Schmidt,⁶⁰ M. Schmitt,³⁸ T. Schwarz,⁷ L. Scodellaro,¹¹ A. L. Scott,¹⁰ A. Scribano,⁴⁶ F. Scuri,⁴⁶ A. Sedov,⁴⁸ S. Seidel,³⁷ Y. Seiya,⁴¹ A. Semenov,¹⁵ L. Sexton-Kennedy,¹⁷ A. Sfyrla,²⁰ S. Z. Shalhout,⁵⁸ M. D. Shapiro,²⁹ T. Shears,³⁰ P. F. Shepard,⁴⁷ D. Sherman,²² M. Shimojima,^{55,k} M. Shochet,¹³ Y. Shon,⁵⁹ I. Shreyber,²⁰ A. Sidoti,⁴⁶ P. Sinervo,³⁴ A. Sisakyan,¹⁵ A. J. Slaughter,¹⁷ J. Slaunwhite,³⁹ K. Sliwa,⁵⁶ J. R. Smith,⁷ F. D. Snider,¹⁷ R. Snihur,³⁴ M. Soderberg,³⁵ A. Soha,⁷ S. Somalwar,⁵² V. Sorin,³⁶ J. Spalding,¹⁷ F. Spinella,⁴⁶ T. Spreitzer,³⁴ P. Squillacioti,⁴⁶ M. Stanitzki,⁶⁰ A. Staveris-Polykalas,⁴⁶ R. St. Denis,²¹ B. Stelzer,⁸ O. Stelzer-Chilton,⁴² D. Stentz,³⁸ J. Strologas,³⁷ D. Stuart,¹⁰ J. S. Suh,²⁸ A. Sukhanov,¹⁸ H. Sun,⁵⁶ I. Suslov,¹⁵ T. Suzuki,⁵⁵ A. Taffard,^{24,p} R. Takashima,⁴⁰ Y. Takeuchi,⁵⁵ R. Tanaka,⁴⁰ M. Tecchio,³⁵ P. K. Teng,¹ K. Terashi,⁵⁰ J. Thom,^{17,d} A. S. Thompson,²¹ E. Thomson,⁴⁵ P. Tipton,⁶⁰ V. Tiwari,¹² S. Tkaczyk,¹⁷ D. Toback,⁵³ S. Tokar,¹⁴ K. Tollefson,³⁶ T. Tomura,⁵⁵ D. Tonelli,⁴⁶ S. Torre,¹⁹ D. Torretta,¹⁷ S. Tourneur,⁴⁴ W. Trischuk,³⁴ S. Tsuno,⁴⁰ Y. Tu,⁴⁵ N. Turini,⁴⁶ F. Ukegawa,⁵⁵ S. Uozumi,⁵⁵ S. Vallecorsa,²⁰ N. van Remortel,²³ A. Varganov,³⁵ E. Vataga,³⁷ F. Vazquez,^{18,i} G. Velev,¹⁷ C. Vellidis,^{46,a} G. Veramendi,²⁴ V. Veszpremi,⁴⁸ M. Vidal,³² R. Vidal,¹⁷ I. Vila,¹¹ R. Vilar,¹¹ T. Vine,³¹ M. Vogel,³⁷ I. Vollrath,³⁴ I. Volobouev,^{29,o} G. Volpi,⁴⁶ F. Würthwein,⁹ P. Wagner,⁵³ R. G. Wagner,² R. L. Wagner,¹⁷ J. Wagner,²⁶ W. Wagner,²⁶ R. Wallny,⁸ S. M. Wang,¹ A. Warburton,³⁴ D. Waters,³¹ M. Weinberger,⁵³ W. C. Wester III,¹⁷ B. Whitehouse,⁵⁶ D. Whiteson,^{45,p} A. B. Wicklund,² E. Wicklund,¹⁷ G. Williams,³⁴ H. H. Williams,⁴⁵ P. Wilson,¹⁷ B. L. Winer,³⁹ P. Wittich,^{17,d} S. Wolbers,¹⁷ C. Wolfe,¹³ T. Wright,³⁵ X. Wu,²⁰ S. M. Wynne,³⁰ A. Yagil,⁹ K. Yamamoto,⁴¹ J. Yamaoka,⁵² T. Yamashita,⁴⁰ C. Yang,⁶⁰ U. K. Yang,^{13,j} Y. C. Yang,²⁸ W. M. Yao,²⁹ G. P. Yeh,¹⁷ J. Yoh,¹⁷ K. Yorita,¹³ T. Yoshida,⁴¹ G. B. Yu,⁴⁹ I. Yu,²⁸ S. S. Yu,¹⁷ J. C. Yun,¹⁷ L. Zanello,⁵¹ A. Zanetti,⁵⁴ I. Zaw,²² X. Zhang,²⁴ J. Zhou,⁵² and S. Zucchelli⁵

(CDF Collaboration)

¹*Institute of Physics, Academia Sinica, Taipei, Taiwan 11529, Republic of China*²*Argonne National Laboratory, Argonne, Illinois 60439, USA*³*Institut de Física d'Altes Energies, Universitat Autònoma de Barcelona, E-08193, Bellaterra (Barcelona), Spain*⁴*Baylor University, Waco, Texas 76798, USA*⁵*Istituto Nazionale di Fisica Nucleare, University of Bologna, I-40127 Bologna, Italy*⁶*Brandeis University, Waltham, Massachusetts 02254, USA*⁷*University of California, Davis, Davis, California 95616, USA*⁸*University of California, Los Angeles, Los Angeles, California 90024, USA*⁹*University of California, San Diego, La Jolla, California 92093, USA*¹⁰*University of California, Santa Barbara, Santa Barbara, California 93106, USA*¹¹*Instituto de Física de Cantabria, CSIC-University of Cantabria, 39005 Santander, Spain*¹²*Carnegie Mellon University, Pittsburgh, Pennsylvania 15213, USA*¹³*Enrico Fermi Institute, University of Chicago, Chicago, Illinois 60637, USA*¹⁴*Comenius University, 842 48 Bratislava, Slovakia; Institute of Experimental Physics, 040 01 Kosice, Slovakia*¹⁵*Joint Institute for Nuclear Research, RU-141980 Dubna, Russia*¹⁶*Duke University, Durham, North Carolina 27708, USA*¹⁷*Fermi National Accelerator Laboratory, Batavia, Illinois 60510, USA*¹⁸*University of Florida, Gainesville, Florida 32611, USA*¹⁹*Laboratori Nazionali di Frascati, Istituto Nazionale di Fisica Nucleare, I-00044 Frascati, Italy*²⁰*University of Geneva, CH-1211 Geneva 4, Switzerland*²¹*Glasgow University, Glasgow G12 8QQ, United Kingdom*²²*Harvard University, Cambridge, Massachusetts 02138, USA*²³*Division of High Energy Physics, Department of Physics, University of Helsinki and Helsinki Institute of Physics, FIN-00014, Helsinki, Finland*²⁴*University of Illinois, Urbana, Illinois 61801, USA*

- ²⁵The Johns Hopkins University, Baltimore, Maryland 21218, USA
- ²⁶Institut für Experimentelle Kernphysik, Universität Karlsruhe, 76128 Karlsruhe, Germany
- ²⁷High Energy Accelerator Research Organization (KEK), Tsukuba, Ibaraki 305, Japan
- ²⁸Center for High Energy Physics: Kyungpook National University, Taegu 702-701, Korea;
Seoul National University, Seoul 151-742, Korea;
SungKyunKwan University, Suwon 440-746, Korea
- ²⁹Ernest Orlando Lawrence Berkeley National Laboratory, Berkeley, California 94720, USA
- ³⁰University of Liverpool, Liverpool L69 7ZE, United Kingdom
- ³¹University College London, London WC1E 6BT, United Kingdom
- ³²Centro de Investigaciones Energeticas Medioambientales y Tecnologicas, E-28040 Madrid, Spain
- ³³Massachusetts Institute of Technology, Cambridge, Massachusetts 02139, USA
- ³⁴Institute of Particle Physics: McGill University, Montréal, Canada H3A 2T8;
and University of Toronto, Toronto, Canada M5S 1A7
- ³⁵University of Michigan, Ann Arbor, Michigan 48109, USA
- ³⁶Michigan State University, East Lansing, Michigan 48824, USA
- ³⁷University of New Mexico, Albuquerque, New Mexico 87131, USA
- ³⁸Northwestern University, Evanston, Illinois 60208, USA
- ³⁹The Ohio State University, Columbus, Ohio 43210, USA
- ⁴⁰Okayama University, Okayama 700-8530, Japan
- ⁴¹Osaka City University, Osaka 588, Japan
- ⁴²University of Oxford, Oxford OX1 3RH, United Kingdom
- ⁴³University of Padova, Istituto Nazionale di Fisica Nucleare, Sezione di Padova-Trento, I-35131 Padova, Italy
- ⁴⁴LPNHE, Universite Pierre et Marie Curie/IN₂P₃-CNRS, UMR7585, Paris, F-75252 France
- ⁴⁵University of Pennsylvania, Philadelphia, Pennsylvania 19104, USA
- ⁴⁶Istituto Nazionale di Fisica Nucleare Pisa, Universities of Pisa, Siena and Scuola Normale Superiore, I-56127 Pisa, Italy
- ⁴⁷University of Pittsburgh, Pittsburgh, Pennsylvania 15260, USA
- ⁴⁸Purdue University, West Lafayette, Indiana 47907, USA
- ⁴⁹University of Rochester, Rochester, New York 14627, USA
- ⁵⁰The Rockefeller University, New York, New York 10021, USA
- ⁵¹Istituto Nazionale di Fisica Nucleare, Sezione di Roma 1, University of Rome “La Sapienza,” I-00185 Roma, Italy
- ⁵²Rutgers University, Piscataway, New Jersey 08855, USA
- ⁵³Texas A&M University, College Station, Texas 77843, USA
- ⁵⁴Istituto Nazionale di Fisica Nucleare, University of Trieste/Udine, Italy
- ⁵⁵University of Tsukuba, Tsukuba, Ibaraki 305, Japan
- ⁵⁶Tufts University, Medford, Massachusetts 02155, USA
- ⁵⁷Waseda University, Tokyo 169, Japan
- ⁵⁸Wayne State University, Detroit, Michigan 48201, USA
- ⁵⁹University of Wisconsin, Madison, Wisconsin 53706
- ⁶⁰Yale University, New Haven, Connecticut 06520, USA
- (Received 15 June 2007; published 30 May 2008)

We search for a third generation vector leptoquark (VLQ_3) that decays to a b quark and tau lepton using the CDF II detector and 320 pb^{-1} of integrated luminosity from the Fermilab Tevatron. Observing a number of events in agreement with standard model expectations, we obtain, assuming Yang-Mills

^aWith visitors from the University of Athens, 15784 Athens, Greece,

^bWith visitors from the University of Bristol, Bristol BS8 1TL, United Kingdom,

^cWith visitors from the University Libre de Bruxelles, B-1050 Brussels, Belgium,

^dWith visitors from Cornell University, Ithaca, NY 14853, USA

^eWith visitors from the University of Cyprus, Nicosia CY-1678, Cyprus,

^fWith visitors from the University College Dublin, Dublin 4, Ireland,

^gWith visitors from the University of Edinburgh, Edinburgh EH9 3JZ, United Kingdom,

^hWith visitors from the University of Heidelberg, D-69120 Heidelberg, Germany,

ⁱWith visitors from Universidad Iberoamericana, Mexico D.F., Mexico,

^jWith visitors from the University of Manchester, Manchester M13 9PL, England,

^kWith visitors from the Nagasaki Institute of Applied Science, Nagasaki, Japan,

^lWith visitors from the University de Oviedo, E-33007 Oviedo, Spain,

^mWith visitors from the University of London, Queen Mary College, London, E1 4NS, England,

ⁿWith visitors from the University of California Santa Cruz, Santa Cruz, CA 95064, USA

^oWith visitors from Texas Tech University, Lubbock, TX 79409, USA

^pWith visitors from the University of California, Irvine, Irvine, CA 92697, USA

(minimal) couplings, the most stringent upper limit on the $VLQ3$ pair production cross section of 344 fb (493 fb) and lower limit on the $VLQ3$ mass of 317 GeV/ c^2 (251 GeV/ c^2) at 95% C.L.

DOI: [10.1103/PhysRevD.77.091105](https://doi.org/10.1103/PhysRevD.77.091105)

PACS numbers: 14.80.-j, 13.85.Rm

Despite its extraordinary success, the standard model (SM) of elementary particles has structural deficiencies. The parallels between the families of quarks and leptons suggest a possible link between these two sectors at higher mass scales. Leptoquarks, therefore, have been proposed as fractionally charged color-triplet bosons carrying both lepton and baryon quantum numbers. Leptoquarks appear in a wide range of models, including SU(5) grand unification [1], superstrings [2], SU(4) Pati-Salam [3], and compositeness models [4].

The various leptoquark states are classified according to the quantum numbers of SM gauge group interactions [5]. At the Tevatron collider, these states would be predominantly pair-produced through quark antiquark annihilation. In general, larger cross sections, and thus better search sensitivities, are predicted for vector (spin 1) than for scalar leptoquarks [6].

We search for third generation vector leptoquark ($VLQ3$) pair production, and assume each $VLQ3$ decays promptly to a b quark and a tau lepton. As the trilinear and quartic couplings between vector leptoquarks and gluons can have model-dependent “anomalous” contributions, we examine two scenarios: one with Yang-Mills couplings, where vector leptoquarks are fundamental gauge bosons of an extended gauge group, and the other with minimal anomalous couplings [6,7]. Previous $VLQ3$ searches have been carried out in experiments at $p\bar{p}$, e^+e^- , and ep colliders [8–11]. Our new results substantially extend the reach beyond the previous limits.

The results reported in this paper are obtained from 320 pb^{-1} of integrated luminosity collected between March 2002 and August 2004 by the CDF II detector [12], operating at the Tevatron $p\bar{p}$ collider. CDF II is a general-purpose particle detector and has a solenoidal charged particle spectrometer, consisting of 7–8 layers of silicon microstrip detectors and a cylindrical drift chamber immersed in a 1.4 T magnetic field, segmented sampling electromagnetic (EM) and hadronic calorimeters, and a set of charged particle detectors outside the calorimeters used to identify muon candidates. We use a cylindrical coordinate system with the z axis along the beam axis, polar angle θ , azimuthal angle ϕ , and pseudorapidity $\eta \equiv -\ln \tan(\theta/2)$. We define $p_T \equiv p \sin\theta$ and $E_T \equiv E \sin\theta$, where p is the momentum measured by the tracking chambers and E is the energy measured by the calorimeters.

This search assumes a branching ratio $\beta \equiv \mathcal{B}(VLQ3 \rightarrow b\tau) = 1$, and considers a signature where the decay products of the $VLQ3$ pair, $\tau^+\tau^-b\bar{b}$, yield two jets from the b quarks, an electron or muon from a leptonically decaying tau, and a hadronically decaying tau (τ_h). We do not

attempt to identify the jets as originating from b quarks, as this degrades the search sensitivity. A three-level trigger system selects events with lepton candidates and charged tracks [13]. These events are then classified as $e\tau_h$ or $\mu\tau_h$ based on the flavor of the leptonic tau decay.

Selected events are required to contain at least one well-identified electron (muon) candidate that passes fully through the fiducial volume of the cylindrical drift chamber, with transverse energy (momentum) $E_T > 10 \text{ GeV}$ ($p_T > 10 \text{ GeV}/c$). To reduce the background due to multi-jet quantum chromodynamics (QCD) events, an isolation requirement is imposed upon the electron or muon candidate. Specifically, the sum of the p_T of all additional tracks within a cone in $\eta - \phi$ space of $\Delta R < 0.4$ around the track direction of the candidate is required to be less than $2 \text{ GeV}/c$, where $\Delta R \equiv \sqrt{(\Delta\eta)^2 + (\Delta\phi)^2}$.

Hadronic tau candidates are formed by matching narrow clusters of calorimeter towers with tracks [14]. Tracks and π^0 candidates are included within the tau candidate if they are within an angle ω_{\max} from the highest p_T track associated with the τ_h , where ω_{\max} depends on the total cluster energy and ranges from 0.05 to 0.17 rad. Tau candidates with one or three tracks are considered. We reconstruct the π^0 candidates as single narrow clusters in a set of strip and wire chambers embedded in the EM calorimeter at the depth where the longitudinal development of EM showers is expected to be maximal. The τ_h candidates are required to have $|\eta| < 1.0$ and $E_T > 15 \text{ GeV}$. The region between the tau selection cone and a larger 0.52 rad cone serves as an isolation annulus that contains no tracks with $p_T > 1 \text{ GeV}/c$ and in which the summed E_T of all π^0 mesons must be less than 0.6 GeV.

To ensure efficient event reconstruction, the electron or muon candidate (ℓ) direction must be separated from the hadronic tau candidate direction by $\Delta R(\tau_h, \ell) > 0.7$. Jet candidates, with $E_T > 15 \text{ GeV}$, are identified in the region $|\eta| < 2.4$ and are required to be separated from the lepton and tau candidates by $\Delta R(\ell/\tau_h, \text{jet}) > 0.8$.

There are a number of SM processes which can mimic the $VLQ3$ signal. The first category consists of background processes which contain a real $e\tau_h$ or $\mu\tau_h$ plus at least two jets. The primary processes are $Z^0/\gamma^* \rightarrow \tau\tau$ plus at least two jets, and $t\bar{t} \rightarrow WbWb$, where one W yields a hadronic tau via $W \rightarrow \tau\nu_\tau$, the other W similarly yields an electron (muon) or leptonically decaying tau, and the two b quarks give jets.

The second category of backgrounds consists of those that include misidentified final state particles. These include $t\bar{t} \rightarrow WbWb$, where a jet from a hadronic W decay can be misidentified as an electron (muon). The processes

$t\bar{t} \rightarrow WbWb$, $Z^0/\gamma^* \rightarrow e^+e^-$ plus jets, and $Z^0/\gamma^* \rightarrow \mu^+\mu^-$ plus jets also contribute as backgrounds when an electron (muon) or jet is misidentified as the τ_h . Events with W plus jets can pass the selection if one of at least three jets is misidentified as the τ_h . Contributions from diboson channels (WW , WZ , and ZZ) plus jets are negligible. The above contributions and their uncertainties are estimated using PYTHIA [15] Monte Carlo simulation and GEANT [16] CDF II detector simulation. Background from multijet QCD can contribute when jets from quarks are misidentified as an electron (muon) or τ_h . Photon plus jets background enters when high- p_T photons convert within the detector and at least one of the resulting electrons appears as a primary electron candidate, while a jet is misidentified as the τ_h . Contributions from both of these sources are estimated directly from the data, using methods described elsewhere [14].

Further event selection reduces the backgrounds. Backgrounds associated with misidentification are reduced by approximately one-half through a requirement of oppositely charged electron (muon) and τ_h candidates, where the charge of the τ_h candidate is defined as the sum of the charges of all constituent tracks. Events consistent with photon conversions and cosmic rays are removed. To reduce contributions from Z boson production, events are rejected if $76 < m(\ell, X) < 106$ GeV/ c^2 , where X can be the tau candidate or a second electron candidate in the $e\tau_h$ channel, or a second muon candidate in the $\mu\tau_h$ channel. We require $\cancel{E}_T > 10$ GeV, where $\cancel{E}_T = |\vec{\cancel{E}}_T|$ [17]. This requirement reduces backgrounds from $Z^0/\gamma^* \rightarrow \tau^+\tau^-$ and multijet QCD processes and is nearly 100% efficient for the signal process. We define H_T as the scalar sum of electron (muon) candidate E_T , tau candidate E_T , event \cancel{E}_T , and the transverse energies of the two highest E_T jet candidates. The requirements on H_T are given below. The final selection requirement is that the event must contain two or more jets.

To simulate $VLQ3$ pair production and decay [18], we have added the production and decay processes to the GRACE [19] matrix element event generator, which calculates amplitudes, and to the GR@PPA [20] interface, which speeds up computations of the interactions of the primary

hadrons. In addition to providing the theoretical cross section, these programs yield events that are processed through TAUOLA [21] to simulate tau decays, PYTHIA [15] to simulate parton showering, fragmentation, and additional particle decays, and GEANT [16] for the full CDF II detector simulation. For the first time, this framework includes helicity amplitudes for the full matrix element at tree level and propagation of helicity information from the leptoquarks to the tau decay products. We use the parton distribution functions (PDFs) CTEQ5L [22], which we evaluate at an energy scale $Q^2 = m_{VLQ3}$. The absence of higher orders in our theoretical cross section calculation likely results in conservative limits.

We determine total selection efficiencies, including factors for triggering, geometrical and kinematic acceptance, particle candidate identification and isolation, and background suppression criteria. The total efficiencies, averaged between the $e\tau_h$ and $\mu\tau_h$ channels, range from about 2.2% (1.4%) to about 6.1% (5.9%) for Yang-Mills (minimal) couplings over the mass range 160 GeV/ c^2 to 400 GeV/ c^2 . The slightly higher acceptances for the Yang-Mills couplings scenario are due to the fact that the leptoquarks and decay products are more central in this case than they are for the minimal couplings case. For the example of $m_{VLQ3} = 320$ GeV/ c^2 and Yang-Mills couplings, the efficiencies for the $e\tau_h$ and $\mu\tau_h$ channels are $(6.0 \pm 0.1)\%$ and $(6.1 \pm 0.1)\%$, respectively.

We define two signal regions. In addition, three side-band control regions in the plane of the number of jets (N_{jets}) versus H_T are used to verify the expected composition of the backgrounds and the distributions for kinematic quantities. The primary signal region (SR_A) has $N_{\text{jets}} \geq 2$ and $H_T > 400$ GeV, and is sensitive to the highest mass leptoquarks. The secondary signal region (SR_B) has $N_{\text{jets}} \geq 2$ and $250 < H_T < 400$ GeV, and adds sensitivity to lower $VLQ3$ masses (down to the previous mass limits). The three control regions are called CR0J, CR1J, and CR2J, where 0J, 1J, or 2J specifies the number of jets (0, 1, or ≥ 2). Regions CR0J and CR1J include the H_T range $H_T > 80$ GeV, while region CR2J is restricted to $80 < H_T < 250$ GeV. Table I shows the expected background contributions in the control and signal regions, as well as

TABLE I. Numbers of events observed in data and estimates for the total background, for the $e\tau_h$ and $\mu\tau_h$ channels, in the control regions (CR0J, CR1J, CR2J) and signal regions (SR_B, SR_A). For the backgrounds, the statistical uncertainty is given first, followed by the systematic uncertainty.

	Data	$e\tau_h$ Background	Data	$\mu\tau_h$ Background
CR0J	129	$122.1 \pm 2.1 \pm 11.3$	129	$147.1 \pm 2.6 \pm 12.3$
CR1J	110	$109.2 \pm 2.3 \pm 9.3$	79	$100.5 \pm 2.5 \pm 6.7$
CR2J	36	$33.4 \pm 1.4 \pm 4.8$	26	$30.6 \pm 1.6 \pm 3.8$
SR _B	5	$3.3 \pm 0.3 \pm 0.5$	3	$2.2 \pm 0.3 \pm 0.3$
SR _A	0	$0.3 \pm 0.1 \pm 0.1$	0	$0.2 \pm 0.1 \pm 0.1$

the number of events observed in all regions. The signal regions are examined only after an *a priori* optimization of the H_T ranges that maximizes signal sensitivity. Control region CR1J in the $\mu\tau_h$ channel contains the largest difference between the expected and observed number of events, with a difference of 1.9 sigma. Figure 1 shows the H_T distributions for the $e\tau_h$ and $\mu\tau_h$ channels, and includes the control region CR2J and the two signal regions.

The dominant sources of systematic uncertainties on the signal efficiencies are the amount of initial state radiation (ISR) and final state radiation (FSR), the tau identification, and the isolation requirements. The ISR and FSR uncertainties, as evaluated by varying the amount of ISR and FSR in simulation, are each approximately 3.7% of the selection efficiency. The tau identification systematic uncertainty, as measured using methods described elsewhere [14], is 3.0% of the selection efficiency and is primarily due to uncertainties in the response of the hadronic calorimeter to charged tracks and uncertainties in the track reconstruction efficiency. Uncertainty in simulating the

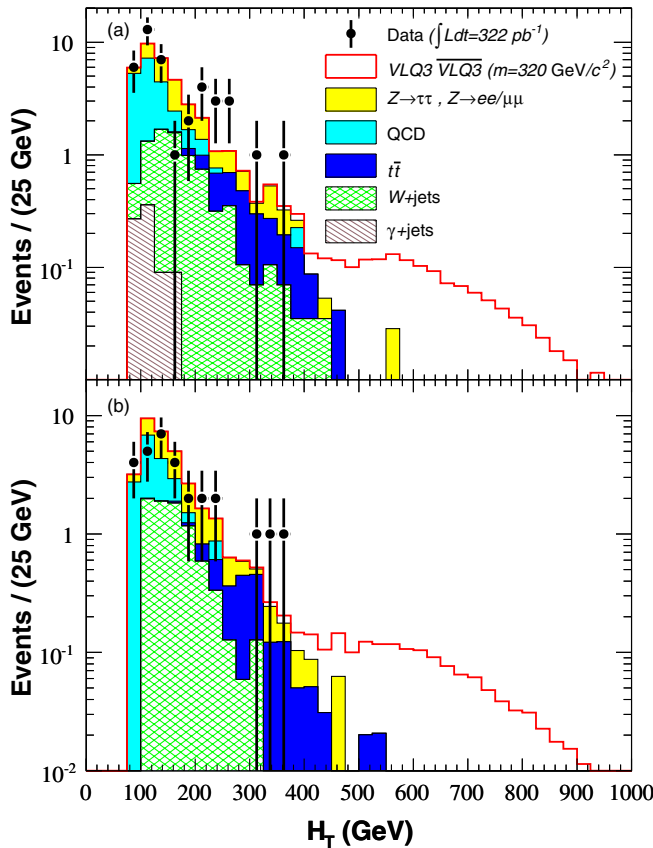


FIG. 1 (color online). Distributions of H_T for the (a) $e\tau_h$ channel and (b) $\mu\tau_h$ channel, including one of the control regions used for validation ($80 < H_T < 250$ GeV), and the regions used for the search ($H_T > 250$ GeV). The individual background contributions are shown, as is a hypothetical signal with mass $m_{VLQ3} = 320$ GeV/ c^2 , normalized to the data sample size.

effect of the lepton isolation requirement is evaluated by comparing the efficiency of this isolation requirement in data and simulation. This yields a 3.0% uncertainty on the selection efficiency. Additional sources of systematic uncertainty on the signal efficiency are the choices of the PDFs and the jet energy scale, as well as smaller contributions from the acceptance criteria, the electron (muon) identification, and the \cancel{E}_T simulation. The total systematic uncertainty on signal efficiency ranges from 10.5% (10.4%) for the $e\tau_h$ ($\mu\tau_h$) channel, for a VLQ3 with mass $m_{VLQ3} = 160$ GeV/ c^2 , down to 7.0% (7.4%) for $m_{VLQ3} = 400$ GeV/ c^2 . The systematic uncertainties on the theoretical prediction of the VLQ3 pair production cross section arise from the choices of PDFs and energy scale Q^2 . These two contributions are combined in quadrature.

A likelihood function is constructed using a Poisson probability distribution of the expected rates of signal plus backgrounds and observed number of events in each channel and signal region. For each VLQ3 mass, the expected signal rates are functions of the VLQ3 pair production cross section. The expected signal rates also include factors for the branching ratios of leptonic and hadronic tau decays, luminosity, and full selection efficiencies. Systematic uncertainties, including 6% due to the luminosity measurement (not included in Table I), are incorporated into the fit. We apply Gaussian probabilities for the uncertainties on the background estimates, and account for correlations among different sources of systematic uncertainties. To set cross section limits for each mass, we integrate the likelihood distribution over all parameters except the cross section, and then integrate as a function of cross section from zero up to the cross section where the integral reaches 0.95.

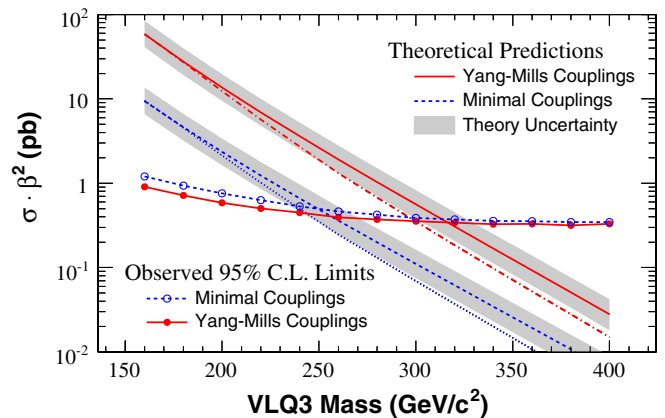


FIG. 2 (color online). The 95% C.L. upper limits on $\sigma(p\bar{p} \rightarrow VLQ3\bar{VLQ3}) \cdot \beta^2$ versus mass (lines with symbols), where $\beta \equiv \mathcal{B}(VLQ3 \rightarrow b\tau)$. The theoretical expectations are shown for the Yang-Mills (solid line) and minimal (dashed line) couplings scenarios for the case $\beta = 1$, with bands for uncertainties due to the choices of PDFs and Q^2 . The dot-dashed and dotted curves show the threshold effect when the $VLQ3 \rightarrow \nu_\tau t$ channel is open.

The results are shown in Fig. 2, as a function of $VLQ3$ mass, along with the leading order theoretical predictions. For a $VLQ3$ with Yang-Mills couplings, at 95% confidence level (C.L.), the upper limit on the cross section is $\sigma < 344$ fb, assuming $\mathcal{B} = 1$, and the lower limit on the mass is $m_{VLQ3} > 317$ GeV/ c^2 . With theoretical uncertainties included on the predicted cross section, the results are $\sigma < 354$ fb and $m_{VLQ3} > 303$ GeV/ c^2 . If decay to $\nu_\tau t$ is allowed [23,24], the mass limit is $m_{VLQ3} > 299$ GeV/ c^2 . For the minimal couplings model, the upper limit on the cross section is $\sigma < 493$ fb and the lower limit on the mass is $m_{VLQ3} > 251$ GeV/ c^2 . With theoretical uncertainties included on the predicted cross section, the results are $\sigma < 555$ fb and $m_{VLQ3} > 235$ GeV/ c^2 . If decay to $\nu_\tau t$ is allowed, the mass limit is $m_{VLQ3} > 238$ GeV/ c^2 . The mass limits are approximately 80–90 GeV/ c^2 higher than those of previous comparable results [8,9].

Using 320 pb $^{-1}$ of luminosity at CDF II, we have searched for $VLQ3$ pair production and subsequent decay to two tau leptons and two jets. We observe no excess of events beyond the expected SM processes and set the most stringent limits to date on the $VLQ3$ mass and pair pro-

duction cross section in the context of two coupling scenarios.

We thank the Fermilab staff and the technical staffs of the participating institutions for their vital contributions. This work was supported by the U.S. Department of Energy and National Science Foundation; the Italian Istituto Nazionale di Fisica Nucleare; the Ministry of Education, Culture, Sports, Science and Technology of Japan; the Natural Sciences and Engineering Research Council of Canada; the National Science Council of the Republic of China; the Swiss National Science Foundation; the A.P. Sloan Foundation; the Bundesministerium für Bildung und Forschung, Germany; the Korean Science and Engineering Foundation and the Korean Research Foundation; the Science and Technology Facilities Council 14 (April 16, 2008) and the Royal Society, UK; the Institut National de Physique Nucleaire et Physique des Particules/CNRS; the Russian Foundation for Basic Research; the Comisión Interministerial de Ciencia y Tecnología, Spain; the European Community's Human Potential Programme; the Slovak R Agency; and the Academy of Finland.

-
- [1] H. Georgi and S.L. Glashow, Phys. Rev. Lett. **32**, 438 (1974).
- [2] J.L. Hewett and T.G. Rizzo, Phys. Rep. **183**, 193 (1989).
- [3] J.C. Pati and A. Salam, Phys. Rev. D **10**, 275 (1974).
- [4] B. Schrempp and F. Schrempp, Phys. Lett. **153B**, 101 (1985).
- [5] W. Buchmuller, R. Ruckl, and D. Wyler, Phys. Lett. B **191**, 442 (1987).
- [6] J.L. Hewett *et al.*, in *Proceedings of the Workshop on Physics at Current Accelerators and Supercolliders, Argonne National Lab*, (Argonne Accel. Phys., Argonne, Illinois, 1993), p. 539.
- [7] J. Blumlein, E. Boos, and A. Kryukov, Z. Phys. C **76**, 137 (1997).
- [8] F. Abe *et al.* (CDF Collaboration), Phys. Rev. Lett. **78**, 2906 (1997).
- [9] B. Abbott *et al.* (D0 Collaboration), Phys. Rev. Lett. **81**, 38 (1998).
- [10] G. Abbiendi *et al.* (OPAL Collaboration), Eur. Phys. J. C **31**, 281 (2003).
- [11] S. Aid *et al.* (H1 Collaboration), Phys. Lett. B **369**, 173 (1996).
- [12] D. Acosta *et al.* (CDF Collaboration), Phys. Rev. D **71**, 032001 (2005).
- [13] A. Anastassov *et al.*, Nucl. Instrum. Methods Phys. Res., Sect. A **518**, 609 (2004).
- [14] A. Abulencia *et al.* (CDF Collaboration), Phys. Rev. D **75**, 092004 (2007).
- [15] T. Sjostrand *et al.*, Comput. Phys. Commun. **76**, 361 (1993); arXiv:hep-ph/0108264. We use version 6.2.
- [16] R. Brun and F. Carminati, CERN Programming Library Long Writeup W5013 (1993).
- [17] The missing transverse energy is defined by $\vec{\cancel{E}}_T = -\sum_i E_T^i \hat{n}_i$, where i = calorimeter tower number with $|\eta| < 3.6$ and \hat{n}_i is a unit vector perpendicular to the beam axis and pointing at the i th calorimeter tower.
- [18] B.C. Allanach *et al.*, arXiv:hep-ph/0602198.
- [19] Minami-Tateya Group, KEK Report No. 92-19, 1993; F. Yuasa *et al.*, Prog. Theor. Phys. Suppl. **138**, 18 (2000).
- [20] S. Tsuno, T. Kaneko, Y. Kurihara, S. Odaka, and K. Kato, Comput. Phys. Commun. **175**, 665 (2006).
- [21] S. Jadach, J.H. Kuhn, and Z. Was, Comput. Phys. Commun. **64**, 275 (1991).
- [22] J. Pumplin *et al.*, J. High Energy Phys. 07 (2002) 012.
- [23] In the case where decay to $\nu_\tau t$ is allowed, the parameter β can be written as $\Gamma_{\tau b}/(\Gamma_{\tau b} + \Gamma_{\nu_\tau t})$. The partial decay widths are $\Gamma_{\tau b} = \frac{p\lambda^2}{4\pi} [2 - (m_\tau^2 + m_b^2)/m_{VLQ3}^2 - (m_\tau^2 - m_b^2)^2/m_{VLQ3}^4 + 6m_\tau m_b/m_{VLQ3}^2]$ and $\Gamma_{\nu_\tau t} = \frac{p\lambda^2}{8\pi} \times [2 - (m_{\nu_\tau}^2 + m_t^2)/m_{VLQ3}^2 - (m_{\nu_\tau}^2 - m_t^2)^2/m_{VLQ3}^4]$, where λ is the coupling constant with fermions and p is the momentum of the relevant decay products in the center of mass frame.
- [24] Note that we do not include the decay of leptoquarks to $\nu_\tau t$ in the background accounting. This leads to slightly conservative limits in the case where decay to $\nu_\tau t$ is allowed.